New Approach to Control SRM Drives

JOSÉ CARLOS QUADRADO
ISEL, R. Cons. Emídio Navarro, 1950-072 LISBOA
CAUTL, Av Rovisco Pais, 1049-001 LISBOA
PORTUGAL

Abstract: - This paper presents a new approach to the control of the turn-on angle used to excite the switched reluctance motor (SRM). The control algorithm determines the turn-on angle that supports the most efficient operation of the motor drive system, and can be divided in two fractions. One fraction of the control algorithm monitors the position of the first peak of the phase current (θ_p) and seeks to align this position with the angle where the inductance begins to increase (θ_m). The second fraction of the controller algorithm monitors the peak phase current and advances the turn-on angle if the commanded reference current cannot be produced by the controller. The first fraction of the controller tends to be active below nominal speed of the SRM, where phase currents can be built easily by the inverter and θ_p is relatively independent of θ_m. The second fraction of the controller is active above nominal speed, where the peak of the phase currents tends to naturally occur at θ_m regardless of the current amplitude. Simulation and experimental results prove that this algorithm provides an efficient operation of the SRM drive.

Key-Words: - SRM, Non-linear control, Electrical drives

1 Introduction

The switched reluctance motor (SRM) produces torque through excitation that is synchronized with the rotor position. The simplest excitation strategy for the SRM is generally described by three excitation parameters: the turn-on angle θ_{on}, the turn-off angle θ_{off}, and the reference current I_{ref}. A control algorithm would typically use the same excitation parameters for each phase, implemented with the spatial shift consistent with the symmetrically displaced phase structure. Control of the excitation angles results in either positive net torque for motoring, or negative net torque for generating. Basic operation of the SRM is given in [1, 2, 3] and the references cited therein.

Efficient operation of the SRM, or any motor drive, is always of importance. Inefficiency leads to larger size, increased weight, and increased energy consumption. The maximization of the SRM efficiency is achieved by maximizing the ratio between the average torque and the RMS phase current, T_{avg}/I_{phRMS}. This ratio measures the achievement of the intended goal of providing the required mechanical output with the minimum electrical input. The proposed approach is valid for drive applications that are tolerant of SRM torque ripple and also for applications that require extremely smooth torque production, though smooth torque production may require current shaping that cannot be characterized by the single parameter I_{ref}.

This present paper presents an excitation angle control algorithm that supports efficient operation of the SRM over its entire speed region. This approach is an alternative to the self-tuning approach to optimization of excitation parameters and to the approach based on the extensive use of look-up tables [4, 5, 6].

2 The Algorithm

The objectives of the proposed algorithm are best explained through consideration of the linear inductance profile for the SRM shown in Fig. 1.

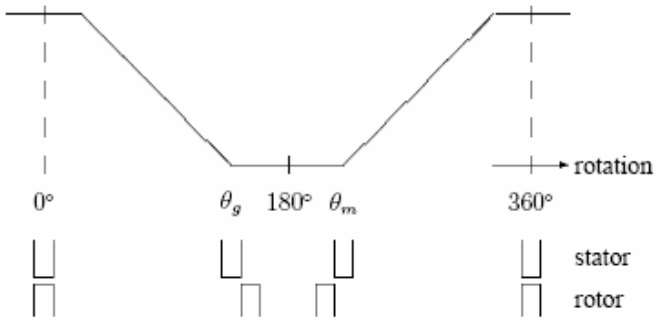

Figure 1: The linear inductance profile of the SRM showing θ_g and θ_m.

In figure 1, the minimum inductance region is defined by the angular interval over which the rotor poles do not overlap the stator poles. Also the maximum inductance region is defined by the angular interval which corresponds to the complete overlap between the stator and rotor poles. The regions of increasing and decreasing inductance correspond to varying overlap between the stator and rotor poles.

For operation as a motor, the SRM phase currents

must be present in the phase winding as the inductance is increasing in the direction of rotation. For operation as a generator, the SRM phase currents must be present in the phase winding as the inductance is decreasing in the direction of rotation. The polarity of current is immaterial, so it is assumed that the phase currents are always positive.

By examining the static torque curve for a typical SRM, it can be observed that the maximum torque for a given amount of current occurs as the rotor begins to move out of the minimum inductance position. This observation suggests that maximum torque per Ampere is produced upon leaving the minimum inductance position.

Iron permeance causes torque production to fall off as overlap between the stator and rotor poles increases. In applications where average torque is of primary importance, it is important to make the most of the region near the unaligned position.

Because it takes time to build the phase currents, the arrival of the torque production region must be foreseen, therefore, it is a must to turn on the phase windings before the angle marked θ_m in Figure 1 to allow the current to be at I_{ref} when the rotor reaches θ_m.

The present approach resorts to simulation results of the experimental SRM drive model. This model must include the SRM magnetic elements to capture the relevant spatial and magnetic nonlinearities that must be considered for a meaningful control design.

Figure 2 shows the motor power output versus the place where the peak current occurs as θ_{on} is varied.

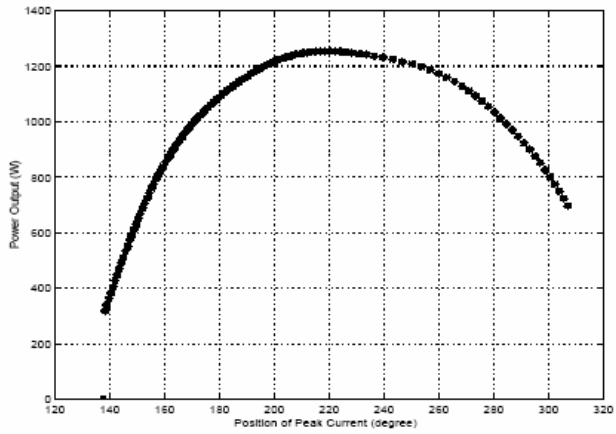

Figure 2: SRM power output as a function of the location where the current first reaches I_{ref}

For the SRM considered in figure 2, θ_m = 225º and θ_g = 135º (electrical), for a speed of 1000 rpm, a I_{ref} = 70 A and conduction angle given by $\theta_{cond} = \theta_{off} - \theta_{on}$ = 145º.

As shown in figure 2, the maximum power is produced when the first peak current occurs at θ_m.

The conventional approach to determining θ_{on} is to work backward from θ_m:

$$\theta_{on} = \theta_m - \frac{L_{\min} I_{ref} \omega}{V_{dc}} \qquad (1)$$

where L_{min} is the minimum inductance value, Vdc is the DC bus voltage, ω is the rotor speed, and I_{ref} is the reference current level.

Equation (1) assumes that the inductance is constant during the region [θ_g, θ_m]. The inductance is in reality a function of the phase current, rotor position and temperature. At low speed this method can give reasonable performance. For operation over a wide speed range (1) starts to break down as the phase back *emf* voltage becomes more prominent. It is desired to have closed loop control that provides the turn-on angle making first peak of the phase current at θ_m without the need of accurate (nonlinear) motor parameters and measurement of the DC bus voltage.

The proposed closed loop control algorithm continuously monitors the position of the first peak of the phase current (θ_p). The turn-on is advanced or retarded automatically according to the error between θ_p and θ_m. This fraction of the controller successfully places θ_p at θ_m. Above base speed the peak current naturally tends to occur near θ_m. At these speeds θ_{on} has little impact on θ_p but significant impact on the magnitude of the current at θ_p. This phenomenon can be observed in figure 3.

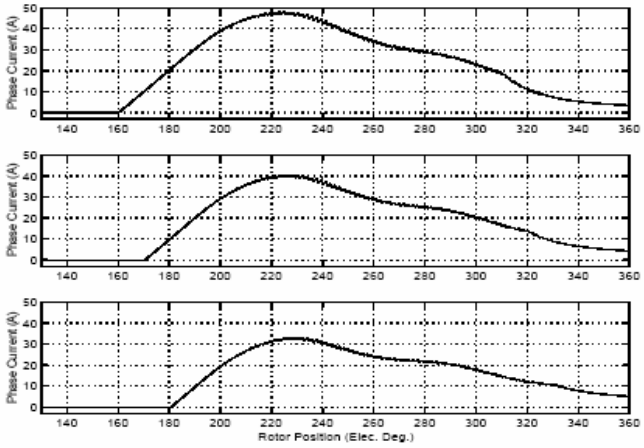

Figure 3: Phase currents at 2500 rpm with different turn-on angles.

In figure 3 the SRM is simulated at 2500 rpm with three different turn-on angles. For each of the turn-on angles, θ_p occurs approximately at the same place with different current magnitudes. To reflect this, the algorithm forces the peak phase current to match the commanded phase current. Feed forward control of θ_{on} using (1) is used to speed convergence to the correct value of θ_{on}. The control of θ_{on} implementation algorithm is summarized in figure 4.

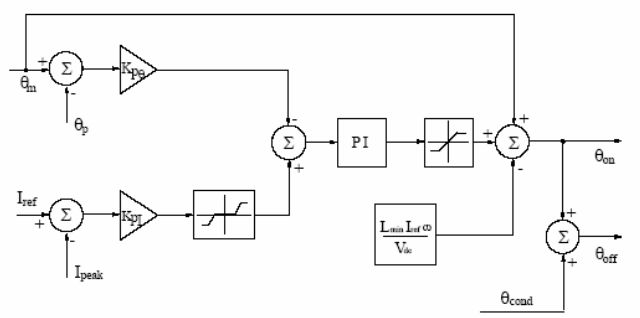

Figure 4: The algorithm used to automatically adjust the turn-on angle

If the controller is in current regulation mode I_p occurs close to I_{ref} so the error between I_p and I_{ref} does not have any effect on the command for θ_{on}. Below base speed, the fraction of the controller responsible for keeping θ_p at θ_m effectively works to achieve the control objective. At high speed if the controller is in voltage control mode θ_p naturally occurs at θ_m. The piece of the controller responsible for forcing I_p to track I_{ref} effectively works to advance the turn on angle to keep I_p close to I_{ref}. If the reference current or the motor speed is reduced the drive enters into current regulation mode and θ_p occurs before θ_m. The piece of the controller responsible for forcing $\theta_p = \theta_m$ becomes active and brings θ_p to θ_m by retarding θ_{on}.

3 Simulation results

The algorithm described in section 2 was simulated to confirm proper operation before being experimentally implemented on the physical system. The SRM to which the simulation is applied is a three-phase SRM designed for a 1kW 42V automotive application. The nominal speed of the SRM is 1000 rpm for an average torque of 10Nm. The aligned phase inductance is 3.77mH; the unaligned phase inductance is 0.32mH. The SRM magnetic elements are modelled analytically [7].

Figure 5 shows the operation of the controller for θ on for operation of the SRM at 1000 rpm with a commanded peak phase current of 70 A.

In figure 5 the controller drives changes in θ_{on} in order to force $\theta_p = \theta_m$ and $I_p = I_{ref}$. At this speed the drive is able to produce the reference current easily and I_p is naturally close to I_{ref} without any control effort. θ_{on} is heavily adjusted by the piece of the control that tries to force $\theta_p = \theta_m$. It is also visible, in figure 5, that the motor average torque production increases as θ_p approaches θ_m. The conduction angle θ_{cond} is maintained at 145º (electrical) for all operating conditions.

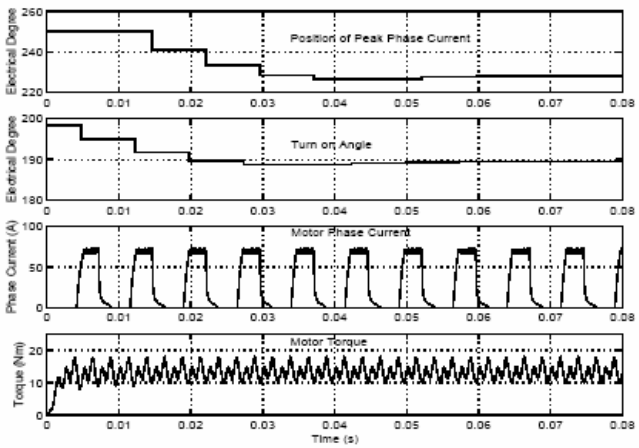

Figure 5: The automatic adjustment of θ_{on} used to drive θ_p to θ_m at 1000 rpm for a 70A reference current.

Figure 6 shows the adjustment of the turn on angle at 2500 rpm. θ_p is close to θ_m throughout operation. The controller objective of keeping θ_p close to θ_m is naturally achieved, while the objective to produce the desired I_{ref} is achieved through the control.

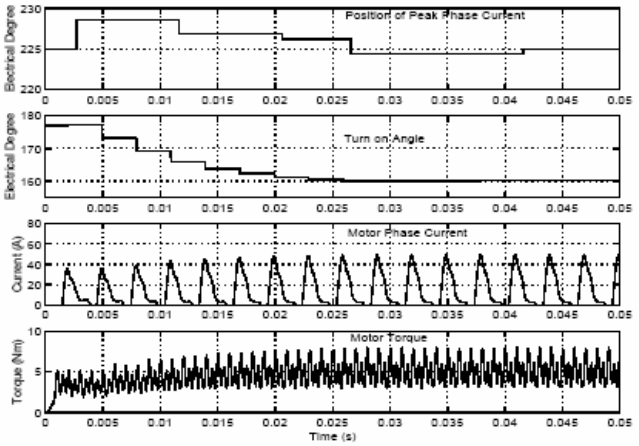

Figure 6: The automatic adjustment of θon used to drive θp to θm at 2500 rpm for a 50A reference current.

Figure 7 shows the transient performance of the controller at 2500 rpm.

In figure 7 the reference current is reduced from 50A to 30A at 0.05 s. The piece of the control responsible for forcing $I_p = I_{ref}$ is unable of sufficiently reducing the advance angle, so the current regulator becomes active. Excessive advance angle does not cause I_p to be greater than I_{ref} because the current regulator prevents the phase current from being greater than I_{ref}. But because θ_p occurs earlier than θ_m, the piece of the controller that is responsible for forcing $\theta_p = \theta_m$ provides effort to reduce the advance angle to the correct value.

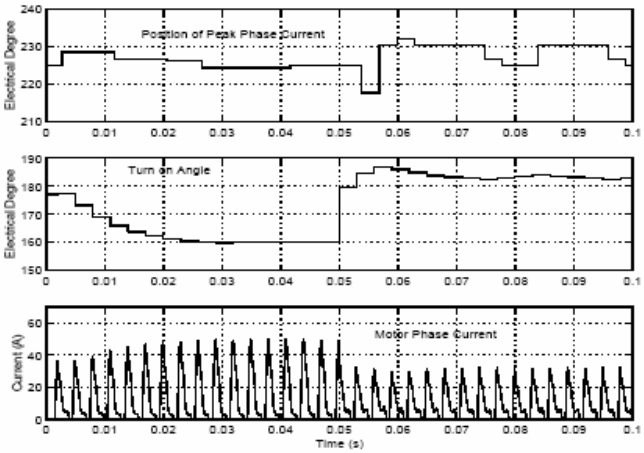

Figure 7: The automatic adjustment of θ_{on} used to drive θ_p to θ_m at 2500 rpm when the reference current is reduced from 50A to 30A at 0.05 s.

4 Experimental results

The performance of the controller is experimentally verified with a three-phase SRM designed for a 1kW 42V automotive application.

The control algorithm of Section 2 was implemented using a digital signal processor. The SRM is coupled to an induction motor, which acts as a constant speed mechanical load through an adjustable speed drive. A shaft encoder provides direct, quadrature and index pulses to the quadrature encoder pulse unit of the DSP. A 42V battery is used throughout the tests to provide dc power to the inverter.

Figure 8 shows a block diagram of the experimental setup for the tests.

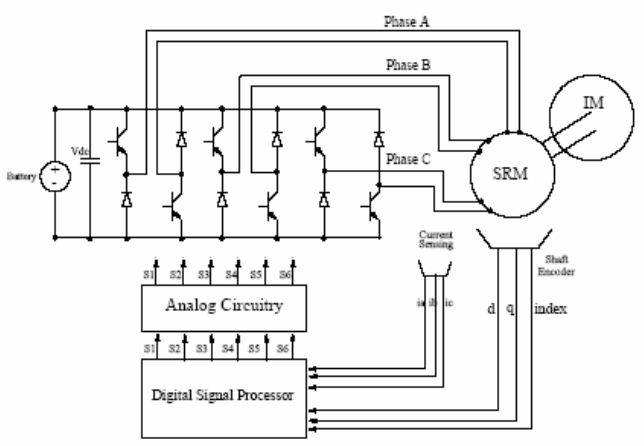

Figure 8: The block diagram of the experimental setup.

Experimental tests were performed at a variety of operating points to show the effectiveness of the controller proposed.

Figure 9 shows the drive performance at 1000 rpm for a 20A reference current with and without the closed loop angle controller.

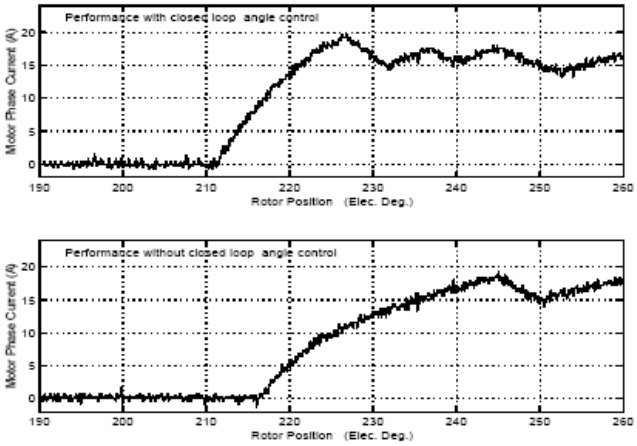

Figure 9: The performance of the experimental system with and without closed loop controller at 1000rpm for a 20A reference current.

In figure 9 the analytically calculated advance angle without closed loop control does not find the advance angle accurately to make $\theta_p = \theta_m$. The closed loop angle controller on the other hand produces the necessary advance angle to make $\theta_p = \theta_m$.

Figure 10 shows a similar test for a 70A reference current. Again performance of the drive is much better with the closed loop angle controller.

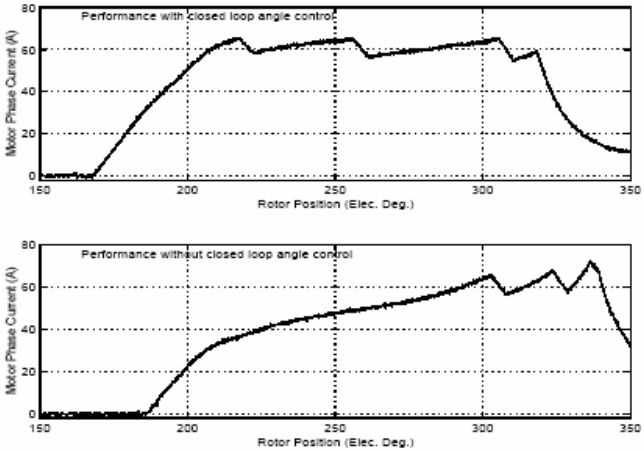

Figure 10: The performance of the experimental system with and without closed loop controller at 1000 rpm for a 70A reference current.

In Figure 10, $\theta_{on} = 168^o$ for closed loop operation and $\theta_{on} = 195^o$ for open loop operation based only on the feed forward value of θ_{on} predicted by (1). The corresponding system efficiencies are 59.1% and 58.8%, respectively. More importantly, the torque values are 9.22Nm and 8.04Nm, respectively. The minor decrease in the efficiency is not surprising given the broad efficiency optimum exhibited by the SRM. However, the electromechanical performance decreases substantially. In fact, the closed loop controller needs to command only 61.7A of phase current to provide 8.04Nm of torque, yielding an

increased system efficiency of 62.7%.
Figure 11 shows the effectiveness of the controller at high speed.

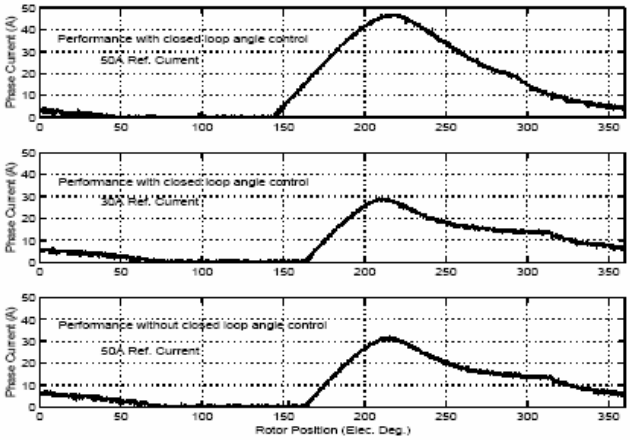

Figure 11: The performance of the experimental system with closed loop controller at 30A and 50A reference currents and without closed loop controller at 50A reference current at 2500 rpm.

The closed loop controller effectively works to make both $\theta_p = \theta_m$ and $I_p = I_{ref}$ at reference currents of 30A and 50 A. The last curve in figure 11 shows the drive response without closed loop control.
The drive without the closed loop control only produces 30A in response to the reference of 50 A. It is worth noticing that peak currents are occurring around the same rotor position independently of the turn on angle and peak current level. The 50A peak current is produced with $\theta_{on} = 137^o$; and the 30A peak current is produced with $\theta_{on} = 169^o$. While the change in system efficiency for these two operating points is small (77.7% versus 77%), there is a substantial change in electromechanical performance. The torque for the 50A reference is 3.22Nm and the torque for the 30A reference is 1.64 Nm. This again suggests that closed loop control of θ_{on} substantially improves drive performance.

5 Conclusion

A new algorithm for the control of θ_{on} has been developed. The new approach provides the turn-on angle adjustment without the need to know the motor parameters and without using self-tuning techniques. The algorithm monitors the peak phase current and where the peak current occurs. It places the position of the first peak of phase current at θ_m in order to maximize the torque per Ampere produced by the SRM. The controller also ensures that the peak phase current is equal to the reference current. The motor, inverter and control system are modelled in Matlab Simulink® to assess the operation of the system. The control technique was then applied to an experimental system. Both simulation and experimental results show that the new control technique provides efficient motor operation with easy implementation and without the need for motor parameters and load conditions.

References:

[1] P. J. Lawrenson, et al., "Variable-speed switched reluctance motors," *IEE Proc.*, Vol. 127, pt. B, no. 4, pp. 253-265, 1980.

[2] T. J. E. Miller, *Switched Reluctance Motors and Their Control*, Oxford, 1993.

[3] R. Krishnan, *Switched Reluctance Motor Drives*, CRC Press, 2001.

[4] B. Fahimi et al., "Self-tuning control of switched reluctance motors for optimized torque per Ampere at all operating points," *Proc. of the IEEE Applied Power Electronics Conf.*, pp. 778-783, 1998.

[5] K. Russa, I. Husain and M. Elbuluk, "A self-tuning controller for switched reluctance motors," *IEEE Trans. on Power Electronics*, Vol. 15, pp. 545-552, 2000.

[6] J.C. Quadrado, "Iterative Approach to Basic Reluctance Motor Control", *WSEAS Trans. On Circuits*, Vol. 1, pp. 119-124, 2002.

[7] D. A. Torrey and J. H. Lang, "Modelling a nonlinear variable reluctance motor drive," *IEE Proc.*, Vol. 137, pt. B, pp. 315-326, 1990.